Astronomy & Astrophysics manuscript no. grb080916C˙aph
June 16, 2013

The redshift and afterglow of the extremely energetic gamma-ray burst GRB 080916C

J. Greiner[1], C. Clemens[1], T. Krühler[1,2], A. v. Kienlin[1], A. Rau[3], R. Sari[4], D.B. Fox[5], N. Kawai[6], P. Afonso[1], M. Ajello[7], E. Berger[8], S.B. Cenko[9], A. Cucchiara[5], R. Filgas[1], S. Klose[10], A. Küpcü Yoldaş[11], G.G. Lichti[1], S. Löw[1], S. McBreen[12,1], T. Nagayama[13], A. Rossi[10], S. Sato[14], G. Szokoly[15,1], A. Yoldaş[1], and X.-L. Zhang[1]

[1] Max-Planck-Institut für extraterrestrische Physik, Giessenbachstrasse 1, 85748 Garching, Germany
e-mail: jcg@mpe.mpg.de
[2] Universe Cluster, Technische Universität München, Boltzmannstraße 2, D-85748, Garching, Germany
[3] Optical Observatories, California Inst. of Technology, 1200 E California Blvd, Pasadena, CA 91125, USA
e-mail: arne@astro.caltech.edu
[4] Dept. of Theor. Astrophysics, California Inst. of Technology, 1200 East California Blvd., Pasadena, CA 91125, USA
e-mail: sari@tapir.caltech.edu
[5] Department of Astronomy & Astrophysics, Pennsylvania State University, 525 Davey Lab, University Park, PA 16802, USA
e-mail: dfox@astro.psu.edu
[6] Dept. of Physics, Tokyo Inst. of Technology, 2-12-1 Ookayama, Meguro-ku, Tokyo 152-8551, Japan
e-mail: nkawai@phys.titech.ac.jp
[7] SLAC/KIPAC, 2575 Sand Hill Road, Menlo Park, CA 94025, USA
e-mail: majello@slac.stanford.edu
[8] Harvard University, 60 Garden Street, Cambridge, MA 02138, USA
e-mail: eberger@cfa.harvard.edu
[9] Department of Astronomy, University of California, Berkeley, CA 94720, USA
e-mail: cenko@astro.berkeley.edu
[10] Thüringer Landessternwarte Tautenburg, Sternwarte 5, D-07778 Tautenburg, Germany
e-mail: klose@tls-tautenburg.de
[11] ESO, Karl-Schwarzschild-Str. 2, 85740 Garching, Germany
e-mail: ayoldas@eso.org
[12] School of Physics, University College Dublin, Belfield, Dublin 4, Ireland
e-mail: sheila.mcbreen@ucd.ie
[13] Dept. of Astronomy, Kyoto University, Sakyo-ku, Kyoto 606-8502, Japan
e-mail: nagayama@kusastro.kyoto-u.ac.jp
[14] Department of Astrophysics, Nagoya University, Furo-cho, Chikusa-ku, Nagoya 464-8602, Japan
e-mail: ssato@z.phys.nagoya-u.ac.jp
[15] Eötvös Univ., 1117 Budapest, Pazmany P. stny. 1/A, Hungary
e-mail: szgyula@elte.hu

Received 22 Dec 2008; accepted 2009

ABSTRACT

Context. The detection of GeV photons from gamma-ray bursts (GRBs) has important consequences for the interpretation and modelling of these most-energetic cosmological explosions. The full exploitation of the high-energy measurements relies, however, on the accurate knowledge of the distance to the events.
Aims. Here we report on the discovery of the afterglow and subsequent redshift determination of GRB 080916C, the first GRB detected by the Fermi Gamma-Ray Space Telescope with high significance detection of photons at energies >0.1 GeV.
Methods. Observations were done with 7-channel imager GROND at the 2.2m MPI/ESO telescope, the SIRIUS instrument at the Nagoya-SAAO 1.4 m telescope in South Africa, and the GMOS instrument at Gemini-S.
Results. The afterglow photometric redshift of $z = 4.35 \pm 0.15$, based on simultaneous 7-filter observations with the Gamma-Ray Optical and Near-infrared Detector (GROND), places GRB 080916C among the top 5 % most distant GRBs, and makes it the most energetic GRB known to date. The detection of GeV photons from such a distant event is rather surprising. The observed gamma-ray variability in the prompt emission together with the redshift suggests a lower limit for the Lorentz factor of the ultra-relativistic ejecta of $\Gamma > 1090$. This value rivals any previous measurements of Γ in GRBs and strengthens the extreme nature of GRB 080916C.

Key words. Gamma rays: bursts – Techniques: photometric

1. Introduction

Long-duration Gamma-Ray Bursts (GRBs) are the high-energy signatures of the death of some massive stars and emit the bulk of their radiation in the 300–800 keV band. In a small number of events, emission up to ∼100 MeV has been detected, e.g., with SMM (Harris & Share 1998), COMPTEL (Hoover et al. 2005), EGRET (Kaneko et al. 2008), and recently with AGILE (Giuliani et al. 2008). These high-energy photons

Table 1. Log of the observations. The first ground-based imaging was obtained with the Simultaneous 3-color (*JHK*) InfraRed Imager for Unbiased Survey (SIRIUS, (Nagayama et al. 2003)) on the Nagoya-SAAO 1.4m telescope (IRSF). GROND, a simultaneous 7-channel imager (Greiner et al. 2008) mounted at the 2.2 m MPI/ESO telescope at La Silla (Chile), started observing about 30.75 hrs after the GRB. The imaging sequence consisted of a series of sixteen 375 s integrations in the $g'r'i'z'$ channels with gaps of about 45 s. In parallel, the JHK_S channels were operated with 10 s integrations, separated by 5 s. Late-time imaging was obtained with the Gemini-South telescope + Gemini Multi-Object Spectrograph (GMOS-South) on 29 Oct 2008, taking eight 180 s exposures. Data reduction was done using IRAF routines. Photometric calibration of the GROND g', r', i', z' bands was performed using the spectrophotometric standard stars SA100-241 and SA97-249, while that of JHK_S was done against 2MASS (Tab. 2).

Date/Time (UT in 2008)	Telescope/Instrument	Filter	Exposure (min)	Brightness (mag)[(a)]
Sep 17 02:53–03:43	IRSF/SIRIUS	JHK_S	50.0	21.0±0.5 / 20.4±0.4 / 20.3±0.5
Sep 17 07:57–09:39	MPI/ESO 2.2m/GROND	$g'r'i'z'$	75.0	>23.6 / 22.81±0.07 / 22.05±0.05 / 21.76±0.05
Sep 17 07:57–09:39	MPI/ESO 2.2m/GROND	JHK_S	60.0	21.50 ± 0.06 / 21.29 ± 0.08 / 21.10 ± 0.15
Sep 19 08:04–09:42	MPI/ESO 2.2m/GROND	$g'r'i'z'$	79.4	> 23.6 / > 23.8 / 23.47 ± 0.13 / > 23.8
Sep 19 08:04–09:42	MPI/ESO 2.2m/GROND	JHK_S	64.0	> 21.9 / > 21.2 / > 20.5
Sep 20 08:42–09:42	MPI/ESO 2.2m/GROND	$g'r'i'z'$	50.0	> 23.9 / > 24.2 / 23.78 ± 0.16 / > 23.8
Sep 20 08:42–09:42	MPI/ESO 2.2m/GROND	JHK_S	40.0	> 22.5 / > 21.5 / > 20.6
Sep 24 07:32–09:31	MPI/ESO 2.2m/GROND	$g'r'i'z'$	100.1	> 25.0 / > 24.5 / > 24.3 / > 23.9
Sep 24 07:32–09:31	MPI/ESO 2.2m/GROND	JHK_S	74.2	> 22.2 / > 21.5 / > 20.8
Oct 29 07:59–08:31	Gemini-S/GMOS	i'	24.0	> 25.1

[(a)] Not corrected for Galactic foreground reddening of E(B-V) = 0.32 mag (Schlegel et al. 1998). All magnitudes are given in the AB system.

Table 2. Local photometric standards within 2′ of the GRB. Calibration of the field in *JHK* was performed using 2MASS stars. The magnitudes of the selected 2MASS stars were then transformed into the GROND filter system and finally into AB magnitudes using J(AB) = J(Vega) + 0.91, H(AB) = H(Vega) + 1.38, K(AB) = K(Vega) + 1.81 (Greiner et al. 2008). Systematic errors are ±0.02 mag for $g'r'i'z'$, and ±0.05 mag for JHK_s.

No	Coordinates (J2000)	g'	r'	i'	z'	J	H	K_S
1	07:59:28.97 -56:38:24.0	17.59±0.01	16.82±0.01	16.50±0.01	16.27±0.01	16.24±0.01	15.98±0.01	16.36±0.01
2	07:59:27.40 -56:40:10.1	17.18±0.01	16.18±0.01	15.79±0.01	15.52±0.01	15.37±0.01	15.00±0.01	15.38±0.01
3	07:59:24.01 -56:37:08.0	17.11±0.01	16.31±0.01	15.98±0.01	15.72±0.01	15.67±0.01	15.40±0.01	15.77±0.01
4	07:59:19.84 -56:39:25.3	17.90±0.01	16.92±0.01	16.54±0.01	16.28±0.01	16.15±0.01	15.84±0.01	16.20±0.01
5	07:59:17.70 -56:37:41.9	18.11±0.01	17.09±0.01	16.71±0.01	16.45±0.01	16.36±0.01	16.02±0.01	16.44±0.01

offer unique access to the physics of GRBs. Firstly, the shape of the spectrum provides direct information about the gamma-ray emission mechanism (Pe'er et al. 2007, Giannios 2008). Secondly, high-energy photons can place tight constraints on the Lorentz factor of the ejecta via the pair-production threshold. Furthermore, in some cases, the origin of the high-energy component differs from that of the low-energy emission (e.g., GRB 941017; (Gonzalez et al. 2003)) or the high-energy photons arrive with a significant time delay (e.g., > 1hr in GRB 940217; (Hurley et al. 1999)). The formation of these properties is far from understood and can only be addressed with an increasing number of bursts with GeV detections. Finally, the search for signatures of absorption against the intergalactic UV background light using the shape of the high-energy spectrum as well as the search for quantum gravity dispersion effects over cosmic distances in the light curve are implications of much broader scientific interest (Abdo et al. 2009).

An important prerequisite to the interpretation of the GeV component of a burst is the accurate knowledge of the distance. Only few of the previously detected GRBs with high-energy emission had identified optical afterglows, as the localization capabilities of high-energy missions were insufficient to facilitate rapid follow-up observations.

The recently launched *Fermi* Gamma-Ray Space Telescope has the ability to localise high energy events using the Large Area Telescope (LAT) and to measure spectra over a large energy range in combination with the Gamma-Ray Monitor (GBM) (8 keV to 300 GeV). The *Swift* satellite (Gehrels et al. 2004) can also slew rapidly to LAT locations and provide positions with arcsec-accuracy by the detection of the X-ray afterglow, facilitating and dramatically enhancing the likelihood of a distance measurement.

The bright GRB 080916C was detected by the GBM on 2008 Sep 16th, at 00:12:45 UT (Goldstein & van der Horst 2008). The burst was located in in the field of view of the LAT and emission above 100 MeV was quickly localized (Tajima et al. 2008). Follow-up observations with the *Swift* X-ray telescope (XRT) provided an X-ray afterglow candidate (Kennea 2008) which subsequently led to the discovery of a faint optical/NIR source with GROND (Clemens et al. 2008a) and SIRIUS (Nagayama 2008). Further monitoring in both X-rays (Stratta et al. 2008) and in the optical (Clemens et al. 2008b) established the fading and confirmed the source to be the afterglow of GRB 080916C.

GRB 080916C was also detected by other satellites in addition to Fermi (Hurley et al. 2008): AGILE (MCAL, SuperAGILE, and ACS), RHESSI, INTEGRAL (SPI-ACS), Konus-Wind, and MESSENGER. The preliminary analysis of the GBM integrated spectrum over a duration (T_{90}) of 66 s results in a best fit Band function (Band et al. 1993) with E_{peak} = 424±24 keV, a low-energy photon index α = –0.91±0.02, and a high-energy index β = –2.08±0.06, giving

a fluence of 1.9×10^{-4} erg cm^{-2} in the 8 keV – 30 MeV range (van der Horst & Goldstein 2008). The spectral results reported by RHESSI and Konus-Wind (Golentskii et al. 2008) are in broad agreement.

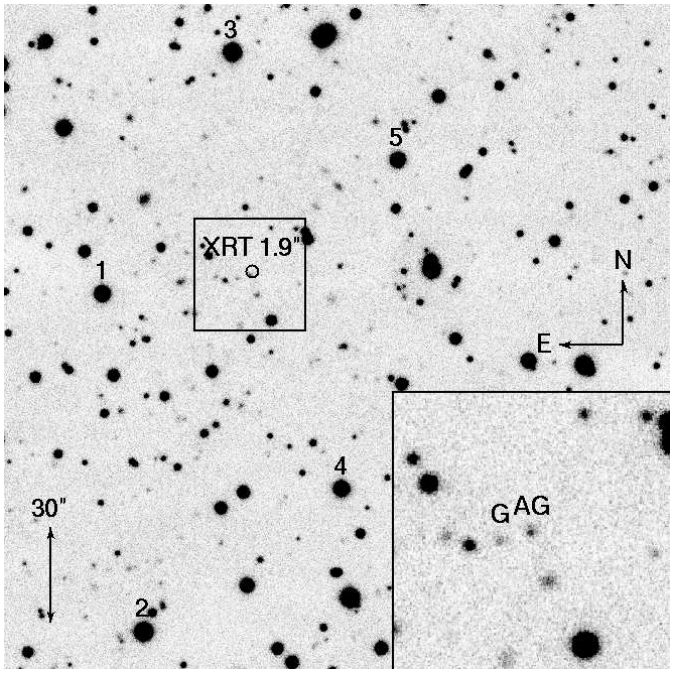

Fig. 1. i'-band image of the afterglow of GRB 080916C obtained with the 7-channel imager GROND at the 2.2m telescope on La Silla / Chile 32 hrs after the burst. The circle denotes the *Swift*/XRT error box. Some of the local standard stars of Tab. 2 are labeled. A zoom into the innermost region is shown in the bottom-right, with the afterglow (AG) and a galaxy (G) 4″ from the afterglow labeled.

The measurements of the high-energy emission from GRB 080916C by the instruments of the Fermi Gamma-Ray Space telescope are described in Abdo et al. (2009). Here we report on the discovery of the optical/NIR afterglow of GRB 080916C, the measurement of its redshift, and consequently on the recognition of its extreme explosion energy and the large Lorentz factor of its relativistic outflow.

The GRB afterglow

A comparison of GROND observations from Sep. 17 and 19, 2008 clearly reveals a fading source inside the *Swift*/XRT error box (Fig. 1), with coordinates RA (J2000.0) = $07^{\rm h}59^{\rm m}23\overset{\rm s}{.}32$, Decl. (J2000.0) = –56°38′18.″0 (0.″5 error). The decay between 1.3 to 4 d after the GRB is well described by a single power law with $\alpha_O = 1.40\pm0.05$ (Fig. 2), compatible within the errors to the X-ray decay slope $\alpha_X = 1.29\pm0.09$.

A spectral energy distribution (SED) was constructed using the GROND magnitudes from the first night of observations (Tab. 1). The photometrically calibrated data (Tab. 2) were corrected for the foreground galactic reddening of E(B-V) = 0.32 mag (Schlegel et al. 1998) corresponding to an extinction of A_V = 0.98 mag and fit by an intrinsic power law ($F_\nu \propto \nu^{-\beta}$) plus three different dust models, as well as without extinction (Tab. 3). The i' to K_S band data are best fit with a power law slope of $\beta = 0.38\pm0.20$ and no host-intrinsic extinction. The i' to r' band

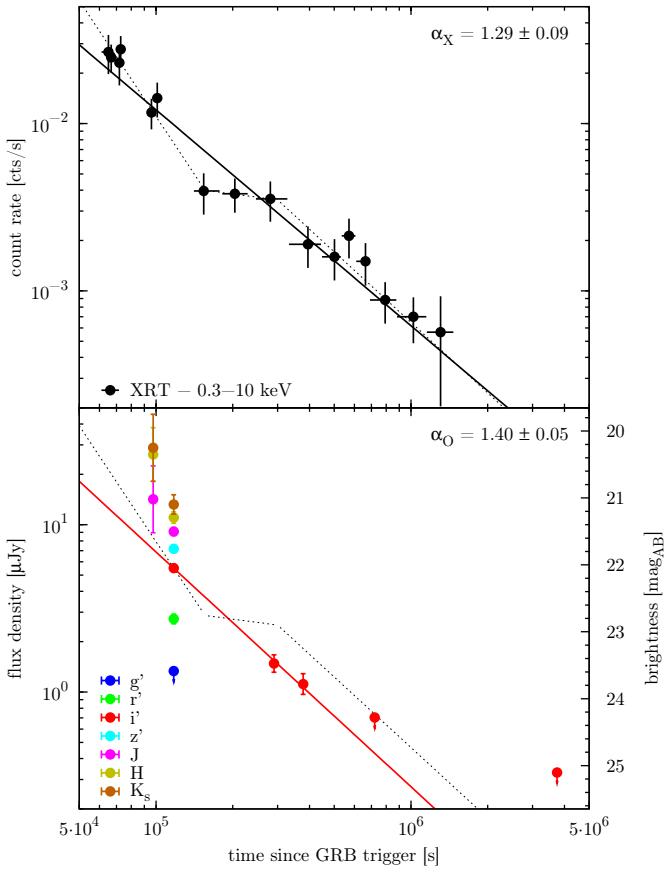

Fig. 2. X-ray (upper panel) and optical/NIR light curve (lower panel) of the GRB 080916C afterglow. The solid lines mark the best fit power laws to the X-ray and i'-band data (labeled in the upper right corner). The power law segments as given by Swift (Stratta et al. 2008) are shown as dashed lines; they were scaled to the i'-band in the lower panel to show that this 3-segment power law does not fit the optical data, i.e. the apparent X-ray plateau phase is not detected in the optical data. However, the X-ray light curve can also be fit with a single power law, with only marginally larger χ^2_{red}, as compared to the 3-segment powerlaw, which results in $\alpha_X = 1.29\pm0.09$, The optical decay is mainly constrained by the three i'-band data points. The JHK_S observations of SIRIUS and GROND during the first night are consistent with this decay.

measurements deviate significantly and can be best explained with a Ly-α break at $z = 4.35\pm0.15$ (see Tab. 3 and Fig. 3, and the rejected alternative explanations given in the figure caption). The redshift values resulting from all the fitted models are compatible, and the redshift error includes already the dependence on the error of the photon index as well as foreground-extinction correction (Fig. 4). The g'-band upper limit is consistent with the high-redshift result, though it is not deep enough to constrain the fit.

No X-ray measurements of the afterglow are available during the time of the initial GROND epoch. However, we can use the SIRIUS JHK_S-band brightness as well as a back-extrapolation of the afterglow decay slope to re-scale the GROND SED to the earlier time when XRT measurements are available. The *Swift*/XRT spectrum from 61–102 ks post-burst has been re-

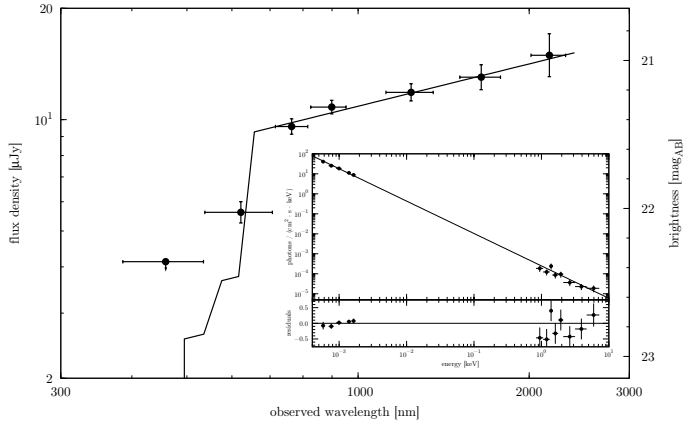

Fig. 3. Spectral energy distribution of the afterglow, derived from the coaddition of all GROND exposures from the first night (Sep. 17, 2008). The SED is best fit with a power law of spectral index $\beta = 0.38$, no extinction, and Lyα absorption at a redshift of $z = 4.35 \pm 0.15$. Alternatively, the r'-band drop could be attributed to reddening in the host galaxy, caused either by substantial UV absorption or a strong broad absorption feature like that at 2175 Å (Krühler et al. 2008). However, the resulting host extinction corrected spectral slope of $\beta \lesssim 0.0$ would be incompatible with most theoretical models (Sari et al. 1998) and with the X-ray spectrum. The lack of curvature in the $i' - K_s$ SED, and its extrapolation to the X-ray data, provides additional arguments against host extinction. Similarly, a spectral break can not easily explain the $r' - i'$ color without redshift as the difference in power law index would be 2.5, much larger than predicted by theory(Sari et al. 1998). In addition, the steep power law would significantly underpredict the observed X-ray fluxes. The inset shows that the best-fit GROND power law connects without break or offset to the Swift/XRT data, supporting the correct modelling of the GROND SED.

Table 3. Results of the spectral energy distribution fitting without dust and with dust models from the Milky Way (MW), Large Magellanic Cloud (LMC), Small Magellanic Cloud (SMC). The redshift and β errors are at the 2σ confidence level.

Dust model	Redshift	β	A_V^{host} (mag)	χ^2_{red}
none	$4.35^{+0.12}_{-0.13}$	$0.38^{+0.20}_{-0.19}$	–	1.04
MW	$4.35^{+0.12}_{-0.16}$	$0.38^{+0.21}_{-0.23}$	$0.0^{+0.4}_{-0.0}$	1.04
LMC	$4.28^{+0.15}_{-0.24}$	$0.34^{+0.19}_{-0.24}$	$0.1^{+0.4}_{-0.1}$	0.95
SMC	$4.35^{+0.13}_{-0.26}$	$0.38^{+0.13}_{-0.28}$	$0.0^{+0.2}_{-0.0}$	1.04

ported to be well fit with an absorbed power law spectrum with photon index $\Gamma_X = 2.1^{+0.9}_{-0.7}$ and a column density of $N_H = 3.7^{+3.3}_{-1.1} \times 10^{21}$ cm^{-2} (Stratta et al. 2008). Using the result of no excess extinction, we re-fit the X-ray spectrum with the column density fixed to the galactic foreground value ($N_H = 1.5 \times 10^{21}$ cm^{-2}), and obtain $\Gamma_X = 1.49^{+0.31}_{-0.34}$, consistent with the slope of the GROND SED (note that the spectral index β is related to the photon index Γ from the X-ray spectral fitting by $\beta_X = \Gamma_X$ - 1). The GROND and XRT combined SED is compatible with a single power law over the complete spectral range (see inset of Fig. 3).

No counterpart or host galaxy was detected seven weeks after the burst at the position of the optical/NIR afterglow, with

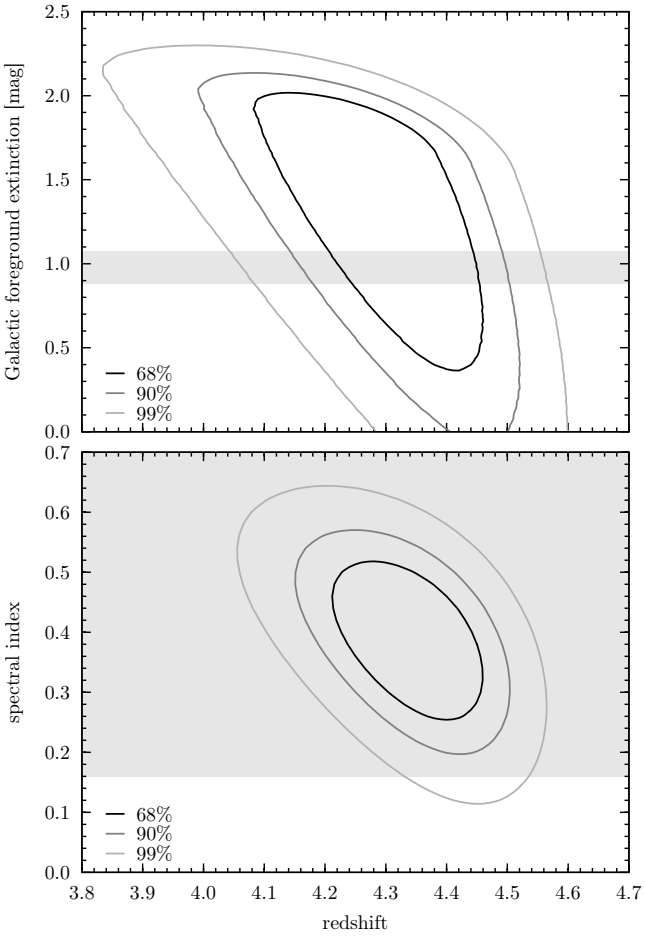

Fig. 4. Contour plot of the foreground A_V (upper panel) and spectral index (lower panel) from the spectral energy distribution fit against the redshift. This shows that the photo-z determination is stable against uncertainties in the correction for the galactic foreground extinction, as well as the powerlaw index. The 68%, 90% and 99% confidence contours are plotted. The shaded area in the upper panel shows the A_V range according to (Schlegel et al. 1998). In the bottom panel the shaded area shows the power-law spectral index from the X-ray spectral fits.

a two-sigma upper limit of $i' > 25.1$ mag within a 1.1″-radius aperture centered at the afterglow position. This is not surprising given the brightness distribution of the known GRB host galaxies (Savaglio et al. 2009); the brightness limit places a loose lower limit on the redshift of $z > 1$.

We note that the nearest object visible on our images is a galaxy at 4″ distance to the East. We obtained an optical spectrum of this galaxy beginning at 05:00 UT on 7 November 2008, using the Gemini-South telescope + GMOS-S. We obtained two spectra of 900 s each with the R400 grating centered at 8000 Å, a second-order blocking filter in place, and with the slit oriented to provide simultaneous coverage of the afterglow position. Observations were carried out at relatively high airmass, with 1.7″ seeing and variable sky background, and consist of two spectra of 900 s each. Bias subtraction, flat-fielding, and wavelength calibration were performed using the GMOS reduction package under the *IRAF* environment. The wavelength so-

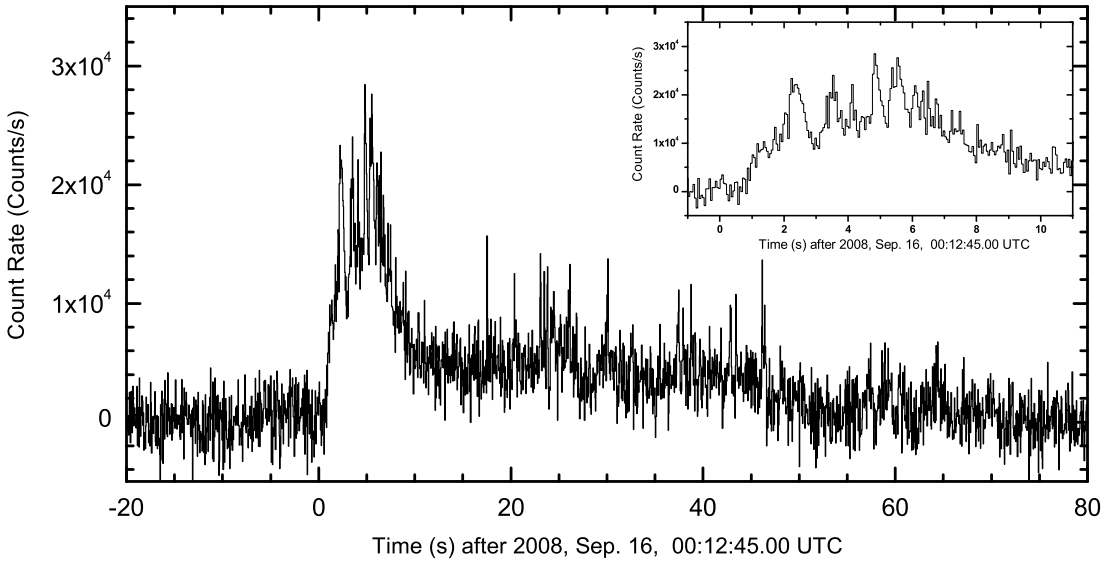

Fig. 5. Prompt emission light curve in the 80 keV–30 MeV energy band as measured with INTEGRAL SPI-ACS at 50 ms resolution. The inset shows a zoom of the main peak. Variability on time scale as short as 100 ms is visible – we measure several 6σ flux variations relative to the neighbouring data bins on the 100 ms time scale.

lution was derived using a CuAr lamp spectrum taken immediately after the science spectra. Following extraction, the two one-dimensional spectra were coadded to increase signal-to-noise, achieving a median S/N of 15.8 over the 6000–10,000 Å wavelength range. We clearly detect the continuum of the resolved galaxy at wavelengths greater than 6100 Å, placing an upper limit on the redshift of this galaxy of $z < 4.0$, based on the absence of Lyman-alpha absorption. This is below the 99% confidence range for the redshift of GRB 080916C (Fig. 4), and thus this galaxy is not related this burst.

Discussion and Conclusions

It is widely believed that long GRBs are produced in the gravitational collapse of a massive star into a neutron star or black hole. It has been argued in the past that the observed total energy in GRBs requires that the emission is relativistic. GRB 080916C is unrivaled by all previous events in this respect: with its observed fluence in the 8 keV–30 MeV band (Hurley et al. 2008), and redshift of 4.35±0.15, its total isotropic energy release is a staggering 6.5×10^{54} erg, corresponding to 4 $M_\odot\times c^2$!

The afterglow decay slope is unlikely a post-jet break decay, which allows one to assume that the jet break occurs after the final XRT observations at 2×10^6 s. A break after this time would place a lower limit on the jet half-opening angle of $6.^\circ1\pm0.^\circ1$ (ISM surrounding with density of 1 cm^{-3}) or $2.^\circ2\pm0.^\circ1$ (wind medium), which in turn implies lower limits for the beaming-corrected energy release of $(3.7\pm0.1)\times10^{52}$ erg (ISM) or $(4.9\pm0.1)\times10^{51}$ erg (wind). While we cannot distinguish between these two cases, we note that the energy for the ISM case is extremely high, exceeding the previous record holders GRB 990123 (6×10^{51} erg) and 050904 (7×10^{51} erg) by several factors. For the wind medium case, a jet break is expected to be very smooth, and might have started near the end of our coverage; thus the real opening angle may not differ much from our lower limit. On the other hand, using our measurements of the decay slope and spectral shape, the cooling frequency would be still above the X-ray band at t ~ 1 d, which is unusual when compared to the majority of GRBs: thus the wind interpretation is less likely than the ISM interpretation.

If the emission were non-relativistic, the required photon field at the burst location would be optically thick to pair-production ("compactness problem"; Ruderman 1975). It has been recognized that in addition to the annihilation of photons into electron/position pairs, the scattering of photons by either the electron or the positron created in the annihilation process, contributes to the optical depth of high-energy photons (Lithwick & Sari 2001). In fact, this latter limit is in many cases more constraining than the pure annihilation limit.

The most sensitive instrument that detected high-energy photons from GRB 080916C was the anti-coincidence system (ACS) of the spectrometer onboard INTEGRAL (SPI) (Rau et al. 2005). At its native time resolution SPI-ACS recorded at peak more than 1200 counts per 50 ms in the 80 keV–30 MeV energy range. This allowed the detection of variability on time scales as short as 100 ms with high statistical significance (see inset of Fig. 5). Using eq. 9 of Lithwick & Sari (2001) and the photon index of $\beta = -2.08$ as measured from GBM (van der Horst & Goldstein 2008), we estimate a lower limit on the Lorentz factor of the ejecta of $\Gamma > 1090$. The previously highest limit on the Lorentz factor of a GRB with known redshift using this method has been $\Gamma > 410$ (Lithwick & Sari 2001) for GRB 971214 at $z = 3.42$, for which the additional assumption had to be made that the photon spectrum actually extended to very high energies.

Over the last two years, an alternative method to determine the initial Lorentz factor has been employed. This involves using observations of the rising part of optical afterglows to determine when the blast wave has decelerated; the corresponding Lorentz factor at the time of the deceleration is expected to be half of the initial Lorentz factor

Γ_0 (Sari & Piran 1999). This method provided $\Gamma_0 \approx 400$ for GRB 060418 and 060607 (Molinari et al. 2007), $\Gamma_0 = 160$ for GRB 070802 (Krühler et al. 2008), $\Gamma_0 = 120$ for GRB 080129 (Greiner et al. 2009), and $\Gamma_0 = 200$ for GRB 071031 (Krühler et al. 2009). Yet another method is based on the evolution of the thermal emission component in the prompt emission of GRBs (Pe'er et al. 2007), and also provides similarly low values of Γ. It is interesting to note that our lower limit on Γ for GRB 080916C is substantially larger than values determined by other methods. Whether or not this is related to the GeV emission in GRB 080916C remains to be seen.

The high signal-to-noise ratio of the SPI-ACS data is also ideal for estimating the variability of the light curve, a quantity that has been shown to correlate with the isotropic equivalent peak luminosity, $L_{\rm iso,peak}$. Following the method described in Li & Paczyński (2006) and using a smoothing time scale of 13.7 s, we derived a variability index of $V = -2.26$ and a resulting $L_{\rm iso,peak} = (1.23 \pm 0.32) \times 10^{52}$ erg s^{-1} (80 keV–30 MeV). Using the observed 256 ms peak flux from Konus (Golentskii et al. 2008), we derive $L_{\rm iso,peak} = 2 \times 10^{53}$ erg s^{-1} (20 keV–10 MeV).

For the future, the synergy of the detection of GRBs with GeV emission coupled with the ability to localise and determine redshifts for these events will be extremely interesting as both Γ-determination methods can be applied, providing a consistency check of our picture of the GRB and afterglow emission process.

Acknowledgements. TK acknowledges support by the DFG cluster of excellence 'Origin and Structure of the Universe'. Part of the funding for GROND (both hardware as well as personnel) was generously granted from the Leibniz-Prize to Prof. G. Hasinger (DFG grant HA 1850/28-1). AvK acknowledges funding through DLR 50 QV 0301, and XLZ through DLR 50 OG 0502. This work made use of data supplied by the UK Swift Science Data Centre at the University of Leicester.

References

Abdo A.A., Ackermann M., Ajello M., et al. 2009, Science (in press)
Band D., Matteson J., Ford L. et al. 1993, ApJ 413, 281
Clemens C., Rossi A., Greiner J., et al. 2008a, GCN #8257
Clemens C., Rossi A., Greiner J., et al. 2008b, GCN #8272
Gehrels N., Chincarini G., Giommi P., et al. 2004, ApJ 621, 558
Giannios, D., 2008, A&A 488, L55
Giuliani, A., Mereghetti, S., Fornari, F., et al. 2008, A&A 491, L25
Goldstein A., van der Horst A., 2008, GCN #8245
Golenetskii S., Aptekar R., Mazets E., et al. 2008, GCN #8258
Gonzalez M.M., Dingus B.L., Kaneko Y., et al. 2003, Nat. 424, 749
Greiner J., Bornemann W., Clemens C., et al. 2008, PASP 120, 405
Greiner J., Krühler T., McBreen S., et al. 2009, ApJ (in press; arXiv:0811.4291)
Harris, M.J.; Share, G.H. 1998, ApJ 494, 724
Hoover, A.S.; Kippen, R.M.; McConnell, M.L. 2005, Il Nuovo Cimento C28, Issue 4, p.825
Hurley K., Dingus B.L., Mukherjee R., et al. 1994, Nat. 372, 652
Hurley K., Goldsten J., Golenetskii S., et al. 2008, GCN #8251
Kaneko, Y.; Gonzalez, M.M.; Preece, R.D.; et al. 2008, ApJ 677, 1168
Kennea J.A., 2008 , GCN #8253
Krühler T., Küpcü Yoldaş A., Greiner J., et al. 2008, ApJ 685, 376
Krühler T., Greiner J., McBreen S., et al. 2009, ApJ (subm.)
Li, L.-X., Paczyński, B., 2006, MN 366, 219
Lithwick Y., Sari R., 2001, ApJ 555, 540
Molinari E., et al. 2007, A&a 469, L13
Nagayama, T. et al. 2003, Proc. SPIE 4841, p. 459
Nagayama T., 2008 , GCN #8274
Pe'er, A.; Ryde, F.; Wijers, R.A.M.J.; et al. 2007, ApJ 664, L1
Rau, A.; Kienlin, A. V.; Hurley, K.; Lichti, G. G. 2005, A&A 438, 1175
Ruderman M. 1975, Ann. NY Acad. Sci., 262, 164
Sari, R., Piran, T., Narayan, R. 1998, ApJ 497, L17
Sari R., Piran T., 1999, ApJ 520, 641
Savaglio, S.; Glazebrook, K.; Le Borgne, D. 2009, ApJ 691, 182
Schlegel, D., Finkbeiner, D., Davis, M. 1998, ApJ 500, 525
Stratta G., Perri M., Preger B. et al. 2008, GCN Report #166.1
Tajima H., Bregeon J., Chiang J., et al. 2008, GCN #8246
van der Horst A., Goldstein A., 2008, GCN #8278